

# Chemical Differences in Soil Organic Matter Fractions Determined by Diffuse-Reflectance Mid-Infrared Spectroscopy

## Francisco J. Calderón\*

USDA-ARS  
Central Great Plains Res. Strn.  
40335 County Rd. GG  
Akron, CO 80720

## James B. Reeves III

USDA-ARS  
Environmental Management and  
Byproduct Utilization Lab.  
Room 117  
10300 Baltimore Ave.  
Bldg. 308 BARC-EAST  
Beltsville, MD 20705

## Harold P. Collins

USDA-ARS  
Vegetable and Forage Crops  
Research Lab.  
24106 North Bunn Rd.  
Prosser, WA 99350

## Eldor A. Paul

Colorado State Univ.  
Natural Resource Ecology Lab.  
Fort Collins, CO 80523

We performed mid-infrared (MidIR) spectral interpretation of fractionated fresh and incubated soils to determine changes in soil organic matter (SOM) chemistry during incubation. Soils from four sites and three depths were processed to obtain the light fraction (LF), particulate organic matter (POM), silt-sized (silt), and clay-sized (clay) fractions. Our results show that the LF and clay fractions have distinct spectral features regardless of site. The LF is characterized by absorbance at  $3400\text{ cm}^{-1}$ , as well as between  $1750$  and  $1350\text{ cm}^{-1}$ . The clay fraction is distinguished by absorption near  $1230\text{ cm}^{-1}$ , and absorption at  $780$  to  $620\text{ cm}^{-1}$ . The POM, like the LF, absorbs at the broad peak at  $1360\text{ cm}^{-1}$ . High SOM soils are characterized by absorbance at  $1230\text{ cm}^{-1}$ , a band for aromatics, possibly associated with resistant C. Soils from different sampling depths have specific spectral properties. A band at  $1330\text{ cm}^{-1}$  is characteristic of shallow depths. Because of their low organic matter (OM) content, the deeper samples are characterized by mineral bands such as quartz, clays, and carbonate. Spectroscopic data indicates that the clay fraction and the LF suffered measurable chemical transformations during the 800-d incubation, but the POM and silt fraction did not. As the LF decomposes, it loses absorbance at  $3400$ ,  $1223$ , and  $2920$  to  $2860\text{ cm}^{-1}$ . The band at  $1630\text{ cm}^{-1}$  increased during incubation, suggesting a resistant form of organic C. The clay fraction suffered changes that were opposite to those of the LF, indicating that LF decomposition and clay decomposition follow different chemistries.

**Abbreviations:** KBS, W.K. Kellogg Biological Station; LF, light fraction; MidIR, mid-infrared; MRT, mean residence time; OM, organic matter; POM, particulate organic matter; Py-MBMS, pyrolysis-molecular beam mass spectrometry; SOC, soil organic carbon; SOM, soil organic matter.

Understanding SOM composition and cycling is fundamental because SOM contains large nutrient pools for crop growth, affects the soil physical properties necessary for roots to thrive, and can serve as a source or a sink for atmospheric  $\text{CO}_2$  (Lal, 2004). The stability of soil organic carbon (SOC) is determined by interactive effects of climate, parent material, soil depth, and agronomic management (Collins et al., 2000), and there is still much to be learned about OM quality and dynamics.

One approach to the study of SOM quality is fractionation by particle size and settling characteristics. The fractions consist of the LF made up of low density plant material, the POM included with the sand-sized material and protected C in aggregates, and the silt (silt) and clay-size (clay) separates (Haile-Mariam et al., 2008). Soil fractionation has given insight into the complexity of SOM, uncovering a range of C age, N content, and chemical makeup (Paul et al., 2001). In Corn Belt soils, the LF and POM contain relatively labile C and can comprise up to 5 and 11% of the SOC, respectively (Haile-Mariam et al., 2008). The LF contains plant residues and has a shorter C turnover time than the other particle-size fractions. In contrast, the silt and clay fractions tend to have more recalcitrant C than the other fractions (Christensen, 1987).

Extended laboratory incubations help characterize soils because the active C pools are transformed by microbial enzymes while the resistant SOC is less affected

Soil Sci. Soc. Am. J. 75:568–579  
Posted online 18 Jan. 2011  
Open Access Article  
doi:10.2136/sssaj2009.0375  
Received 1 Oct. 2009.

\*Corresponding author (francisco.calderon@ars.usda.gov).

© Soil Science Society of America, 5585 Guilford Rd., Madison WI 53711 USA

All rights reserved. No part of this periodical may be reproduced or transmitted in any form or by any means, electronic or mechanical, including photocopying, recording, or any information storage and retrieval system, without permission in writing from the publisher. Permission for printing and for reprinting the material contained herein has been obtained by the publisher.

deciduous hardwood forest, while the Lamberton Minnesota soils developed under grassland. Wooster, KBS, and Lamberton were started in agriculture in the 1800s, while Hoytville was not cultivated until the early 20th century once drainage issues were resolved. All four sites had been in continuous corn for at least 8 yr before sampling.

Six cores (5.4 cm) were collected from each site to a depth of 1 m and depth sections were composited to make each field replicate. Four replicates were obtained from Lamberton and KBS, and three replicates from Wooster and Hoytville. The samples were sieved (2 mm) and plant debris was excluded. For this experiment, three depth increments were analyzed: 0 to 20, 25 to 50, and 50 to 100 cm. A subset of soil samples was acidified to remove carbonates by mixing 20 g of soil with 100 mL of 250 mM HCl, shaking for 1 h, then washing three times with de-ionized water. The samples were centrifuged, dried at 55°C, and ground (180  $\mu\text{m}$ ). This resulted in soluble organic C losses of up to 10% (Haile-Mariam et al., 2008). Additional details about the sites, sampling, and analysis can be found in Collins et al. (2000).

Soil samples from the 0- to 20-cm depth were separated into particle-size fractions. The LF was obtained by mixing 10 g of soil with 40 mL of NaI solution (1.70 g  $\text{cm}^{-3}$  specific gravity), then the floating material was dried and ground before scanning. The soil material remaining after extracting the LF was rinsed three times with water, then shaken for 15 h in 30 mL of 5 g  $\text{L}^{-1}$  sodium hexametaphosphate. The POM plus sand was obtained by sieving (53  $\mu\text{m}$ ) the dispersed samples. The material retained in the sieve was then dried at 60°C overnight. The silt and clay were obtained by sedimentation and decantation of the material that passed through the 53- $\mu\text{m}$  sieve.

The laboratory incubations were done with 25-g samples (0- to 20-cm depth) of each field replicate (Collins et al., 2000). The samples were brought to 60% of water holding capacity and stored in the dark. The incubation was designed to sample headspace  $\text{CO}_2$ , so the containers were opened initially every 10 d, and later every  $\sim 21$  d. After each  $\text{CO}_2$  sampling, each container was restored to ambient  $\text{CO}_2$  with compressed air. After the incubation, each soil sample was air dried until fractionation using the above procedures (Haile-Mariam et al., 2008). Only the fraction samples (LF, POM, silt, and clay) were available after incubation.

All soil and soil fraction samples were scanned undiluted in MidIR on a Digilab FTS 7000 Fourier transform spectrometer (Varian, Inc., Palo Alto, CA) with a deuterated, Peltier-cooled, triglycine sulfate detector and potassium bromide beam splitter. The spectrometer was fitted with a Pike AutoDIFF diffuse reflectance accessory (Pike Technologies, Madison, WI) and KBr was used as background. Data was obtained as pseudo-absorbance ( $\log [1/\text{Reflectance}]$ ). Spectra were collected at 4  $\text{cm}^{-1}$  resolution, with 64 co-added scans per spectrum from 4000 to 400  $\text{cm}^{-1}$ . Duplicate scans of each sample were performed and included in the multivariate analyses.

Shallow (0–20 cm) and deep (50 cm plus) samples of whole soil from each of the four sites were scanned before and after ashing at 550°C for 3 h. We used GRAMS/AI software, Version 7.02 (Thermo Galactic, Salem, NH) to perform spectral subtraction of ashed from un-ashed samples, to bring out the OM spectral features and differentiate them from the mineral features (Cox et al., 2000, Sarkhot et al., 2007).

The whole sample set consisted of 354 samples, which included the different fractions, incubation times, and depths. Spectral differences

between the sites, depths, decalcification, and fraction treatments were determined by principal components analysis (PCA) using the PLS Plus/IQ software in GRAMS/AI Ver. 7.02 (Thermo Galactic, Salem, NH). All spectra were mean-centered and were pretreated with multiplicative scatter correction before the PCA analyses. The PCA scores were used for dimensionality reduction, while the component loadings were used to indicate which spectral bands explained the distribution of the sample scores along the principal components.

## RESULTS AND DISCUSSION

### Whole Soil and Fraction Spectra, Lamberton Site

Data from the different fractions of the Lamberton site are displayed in Fig. 1 to show the appearance of the spectral features in the neat samples. The sharp peak at 3622  $\text{cm}^{-1}$  indicates hydroxyl stretching in clays (Nguyen et al., 1991), and as expected, is prominent in the clay fraction. It is interesting that the LF absorbs in this region, forming a shoulder below the clay fraction. The broad band at 3400  $\text{cm}^{-1}$ , pronounced in the LF, is due to OH or NH stretching typical in crop residues (Haberhauer and Gerzabek, 1999). The LF contributes 0.5 to 0.8 g C  $\text{kg}^{-1}$  and makes up 3 to 5% of the SOC, and isotope analysis has shown that the LF is an active fraction that contains recent plant residue C (Haile-Mariam et al., 2008). The feature between 2950 and 2870  $\text{cm}^{-1}$  is attributed to aliphatic CH stretching (Janik et al., 2007). A series of three peaks between 2000 and 1790  $\text{cm}^{-1}$ , present in the whole soil, silt fraction, and POM, but absent in the LF, mark the presence of quartz in sand (Nguyen et al., 1991). The 1700 to 1250  $\text{cm}^{-1}$  spectral region has concentrated information about many important functional groups. This region indicates differences between the soil fractions, as well as the general similarity between the POM and the silt (Fig. 1). The feature near 1730 to 1700  $\text{cm}^{-1}$  is due to esters and carboxylic acids (Haberhauer and Gerzabek 1999; Cox et al., 2000; Janik et al., 2007; Sarkhot et al., 2007). It forms a shoulder on the stronger broad band at 1650  $\text{cm}^{-1}$  in the LF, although it leads to a peak near 1690  $\text{cm}^{-1}$  in the POM and silt fractions (Fig. 1).

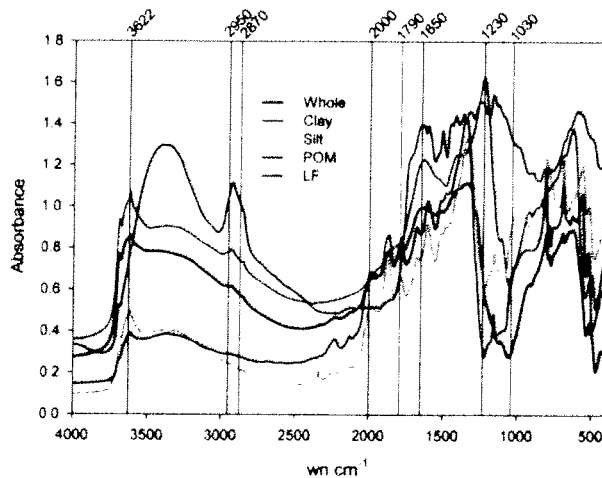


Fig. 1. Mid-infrared spectra of unincubated whole soil and particle size fractions (0–20 cm depth) from Lamberton, MN. POM, particulate organic matter; LF, light fraction; wn, wavenumbers in  $\text{cm}^{-1}$ .

1238  $\text{cm}^{-1}$  could be due to aromatic-CH in plane deformation and has high partial least squares regression loadings for TOC (Janik et al., 2007). This band could also be due to lignin and carbohydrate C-O bands.

Spectral interpretation is challenging between 1400 and 400  $\text{cm}^{-1}$  because bands could be due to several mineral or organic chemicals (Fig. 2). Janik et al. (1998) assign peaks below 1300  $\text{cm}^{-1}$  to kaolinite and quartz, but Janik et al. (2007) indicate that peaks in the <1400  $\text{cm}^{-1}$  region could also be suggestive of cellulose or lignin. Spectral subtraction shows that the aromatic ring CH band at 1238 to 1230  $\text{cm}^{-1}$  may actually be a mineral band in low OM soils (Fig. 2). The Lamberton and Hoytville soils absorb between 1030 and 1160  $\text{cm}^{-1}$  as an organic band, whereas the KBS and Wooster have mineral bands in this region (Fig. 2). Sarkhot et al. (2007) found absorbance at 1160  $\text{cm}^{-1}$  band in soil aggregates. The bands below 1000  $\text{cm}^{-1}$  are mostly mineral in the low SOM KBS and Wooster soils. Lamberton and Hoytville, however, have possibly organic spectral features below 1000  $\text{cm}^{-1}$ . The region from 950 to 700  $\text{cm}^{-1}$  contains many bands due to different linkages in carbohydrates, with a minor influence from lignin and proteins. Janik et al. (1998) found that absorbance at 915  $\text{cm}^{-1}$ , probably due to aromatics and high in the LF (Fig. 1), has high loadings for the prediction of soil C. Our subtraction approach shows that this peak could be due to organic absorption in all four Corn Belt sites (Fig. 2). Spectral subtraction of the near-ashed Lamberton soils shows the following minor peaks that should be organic but cannot be assigned to specific organic bands: 494  $\text{cm}^{-1}$  (present in the clay fraction), and 603 to 598  $\text{cm}^{-1}$  (Fig. 1).

### Comparison of Soil Fractions at Time Zero

Figure 3 shows the PCA of the whole soil and fractions at time zero, for all sites. The PCA indicates that size fractions have spectral differences that override site differences. The POM and silt have similar spectral properties and clustered very closely according to their PCA scores. The clay fraction and the light fraction have distinct spectral properties, forming separate clusters from the rest of the fractions.

The LF has low scores along Component 1, and loadings indicate high absorbance in the following regions: The broad OH/NH band at 3400  $\text{cm}^{-1}$ , the aliphatic and aromatic CH band at 2950 to 2840  $\text{cm}^{-1}$ , the aromatic ring CH band at 1223  $\text{cm}^{-1}$ , and a peak near 490  $\text{cm}^{-1}$  (Fig. 4). These features are prominent in the LF spectrum from the Lamberton site (Fig. 1). The LF also absorbs at the O-Si-O quartz inversion region, indicating low quartz content.

Particulate OM makes up 5 to 23% of the SOC, with the smaller proportions in the fine-textured soils at Lamberton and Hoytville (Haile-Mariam et al., 2008). The POM, and to a lesser extent the silt, have high scores along Component 1, opposite to the LF. Loadings indicate that POM and silt differ from LF in

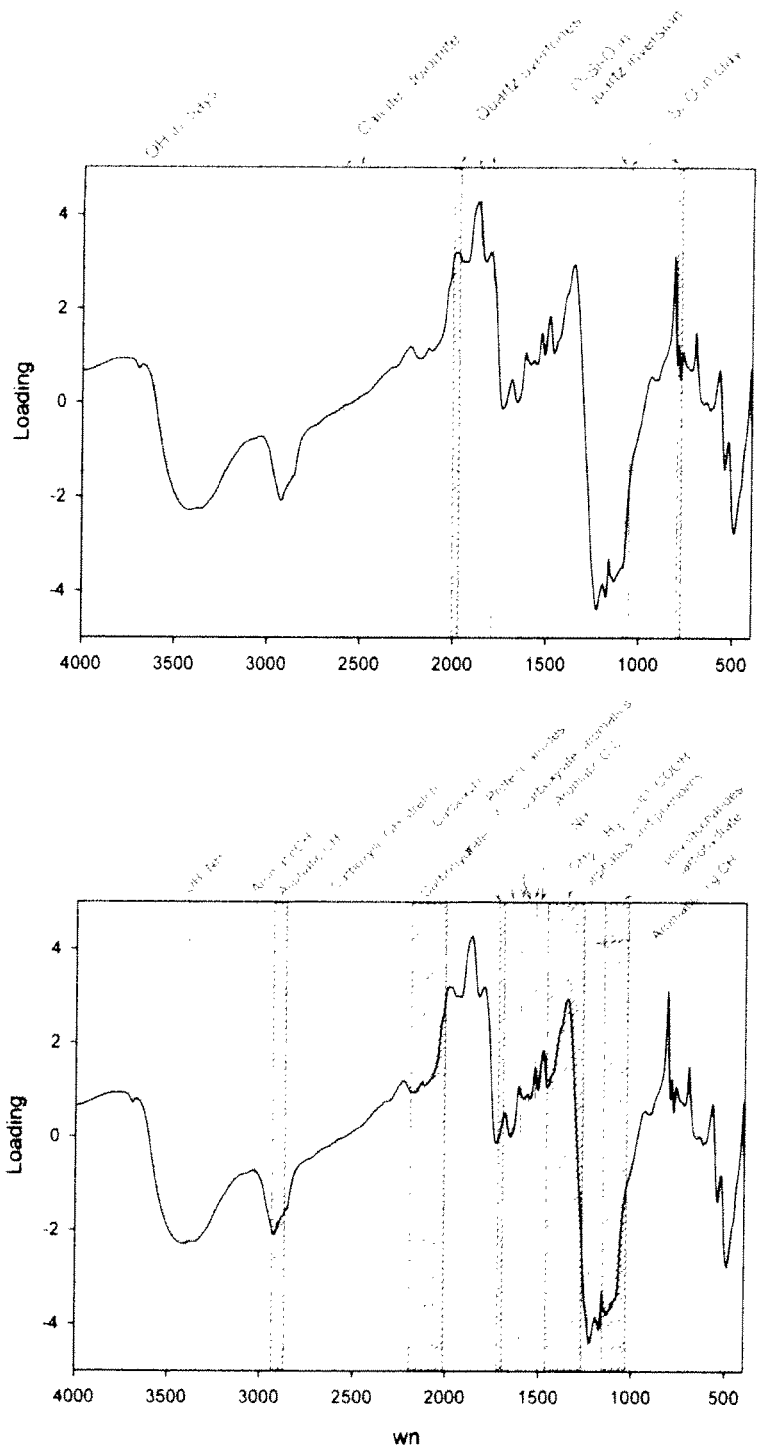


Fig. 4. Component 1 loadings for the principal components analysis of the near mid-infrared spectra of unincubated soil and soil fractions shown in Fig. 3; wn, wavenumbers in  $\text{cm}^{-1}$ . Top graph has the mineral bands indicated, bottom graph has the organic bands.

theories that amino compounds are closely associated with clay surfaces (Sollins et al., 2006). However, we did not find strong spectral amino signals in the clay fraction. The clay samples form two groups in Fig. 3 because the Lamberton clays are spectrally different from the rest of the clays (not shown). This suggests that there are compositional differences between prairie-derived clay from forest-derived clay fractions.

Silt has older C<sub>3</sub>-derived C than the POM (Haile-Mariam et al., 2008, Table 2), yet the POM and silt spectra are relatively similar. A closer look at the PCA in Fig. 3 shows that there are some differences between them. The POM tends to have higher Component 1 scores, and lower Component 2 and 3 scores relative to the silt fraction (Fig. 3). Component loadings indicate that POM has a tendency for higher absorbance than the silt at the broad peak around 1348 cm<sup>-1</sup>, that indicates aliphatics and phenolics. The POM also tends to absorb more than the silt fraction at the 2000 to 1790 cm<sup>-1</sup> quartz band, and at the 3622 cm<sup>-1</sup> clay band (Fig. 4). The silt fraction absorbs higher than the POM at the aromatic ring C-H deformation band near 1223 cm<sup>-1</sup> (Fig. 1 and 6).

### All Sites and Depth, Time Zero Comparison, Unfractionated Soils

The PCA shows that spectral differences between depths are apparent even when all the sites are analyzed together (Fig. 7). Component 3 loadings indicate that the 0- to 20-cm depth absorbs more at the CH bending region near 1330 cm<sup>-1</sup> compared with the deeper soils (data not shown). Figure 2, however, suggests this is possibly a mineral band in the surface soils. The deeper samples, especially those from KBS and Lamberton both have high loadings along Component 3, indicating high absorbance in the quartz overtone region, the 3622 cm<sup>-1</sup> clay band, and the calcite/dolomite band at 2517 cm<sup>-1</sup>.

The PCA in Fig. 7, when coded by site instead of depth, shows that KBS and Wooster samples are separated along Component 2 from the Hoytville and Lamberton samples (not shown). The Lamberton and Hoytville soil are high SOC soils with high clay content, while the KBS and Wooster soils are alfisols of relatively low clay content and low SOC (Paul et al., 2001; Haile-Mariam et al., 2008) (Table 1). Component 2 loadings show that Lamberton and Hoytville absorb highly at 1230 cm<sup>-1</sup> (data not shown). This suggests that this band, high in the clay fraction from Lamberton (Fig. 1) marks samples with high SOC. Note that KBS and Wooster topsoils may have mostly mineral absorption in this region (Fig. 2). Janik et al. (2007) showed that the absorbance at 1230 cm<sup>-1</sup> is characteristic of SOM, and is an important input to total organic C prediction models. Absorbance at 1230 cm<sup>-1</sup> has been attributed to aromatics. However, we did not find that absorbance at 1230 cm<sup>-1</sup> was accompanied by absorbance at 1610 to 1620 cm<sup>-1</sup>, suggesting that this signal represents carbohydrate or more likely mineral clay. Compared with Lamberton and Hoytville soils, KBS and Wooster have low absorbance at the 3622 cm<sup>-1</sup> clay OH band, but absorb highly at the quartz

**Table 2. Characteristics of the Hoytville soil fractions. Data recalculated from Haile-Mariam et al. (2008). MRT = mean residence time.**

	LF	POM	Silt	Clay
0 d C distribution, %	3.5	8.4	23.1	52.9
800 d C distribution, %	1.0	13.8	25.5	50.8
C to N ratio	19.6	15.0	10.3	6.5
0 d <sup>13</sup> C ‰	-14.1	-17.8	-22.4	-23.5
C <sub>3</sub> -C %	16	45	80	89
C <sub>4</sub> MRT yr	3.7	7.8	12.8	26.0
C <sub>3</sub> MRT yr	17.0	38.0	139.0	261.0

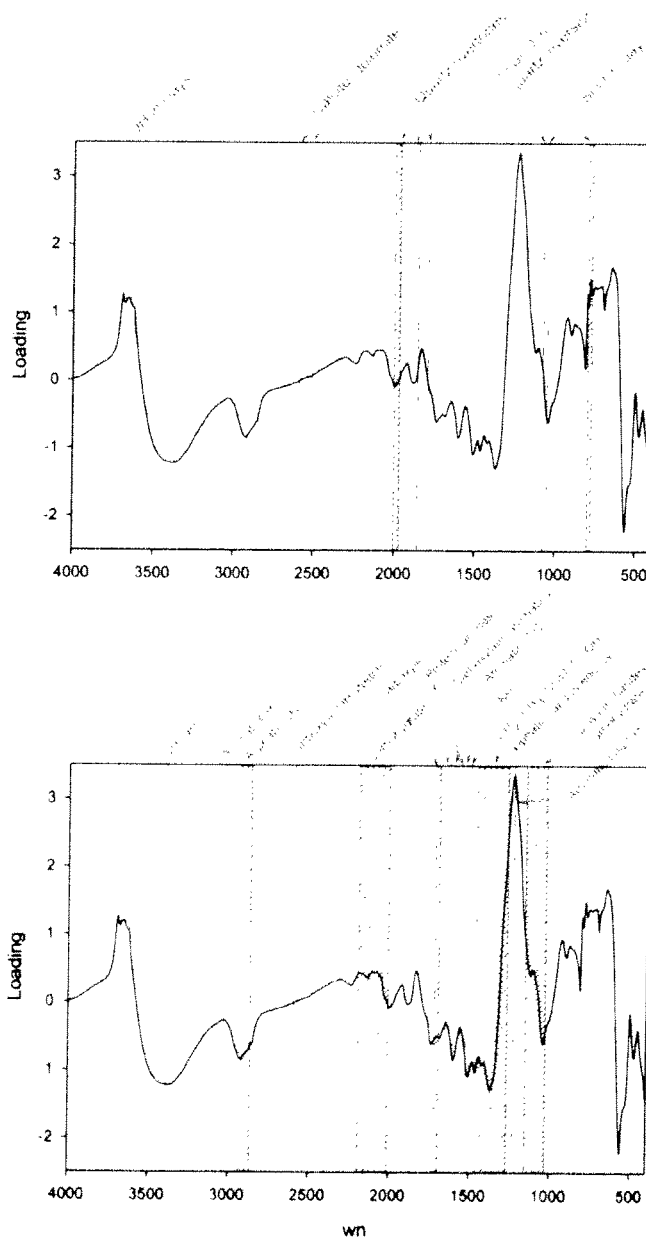


**Fig. 6. Component 3 loadings for the principal components analysis of the neat mid-infrared spectra of unincubated soil and soil fractions shown in Fig. 3; wn, wavenumbers in cm<sup>-1</sup>. Top graph has the mineral bands indicated, bottom graph has the organic bands.**

suggest that humic acids are left over after the easily degraded C is removed. Artz et al. (2006) used the ratio of 1600/1030 (carboxylate/polysaccharide) as an index of decomposition in peat, suggesting that the band near 1630 represents a relatively recalcitrant form of organic C, probably a combination of lignin and humics. The previous study with this set of soils, as exemplified by the data in Table 2, showed that the LF lost more C than the other size fractions, confirming that the LF contains labile plant and microbial material, and can be responsible for short-term soil fertility (Haile-Mariam et al., 2008). The LF C decreased 65% on average during the 800-d incubation, and some of the LF C was transferred to other fractions.

Our spectral analysis showed that the LF fraction contained some clay. We can use previous data from this experiment (Haile-Mariam et al. (2008) to calculate the contribution of the per kilogram clay-associated C3-C to the  $^{13}\text{C}$  value of  $-13.9\text{‰}$  in the LF fraction (Table 2). The LF of this soil had  $360\text{ g C kg}^{-1}$  relative to  $420\text{ g C kg}^{-1}$  in the added corn stover (data not shown). The clay contained  $20\text{ g C kg}^{-1}$ . Thus  $<1\%$  of the C of the LF can be attributed to clay-associated C. This indicates that although LF is shown by MidIR to contain some clay, it also contained other forms of stabilized C not associated with clay. One example could be charcoal. Additional studies are needed to elucidate these observations.

The clay fraction accounts for the largest portion of total soil C in these Corn Belt soils, so changes in clay C quality during laboratory incubation could have important implications for large-scale soil C dynamics. There was a change in SOC distribution during the incubation with a drop in both the LF and clay fractions in spite of the fact that the clay has the oldest MRTs for both the corn-derived C4 and original forest-derived C3 components (Table 2). Component 2 of the clay fraction PCA shows

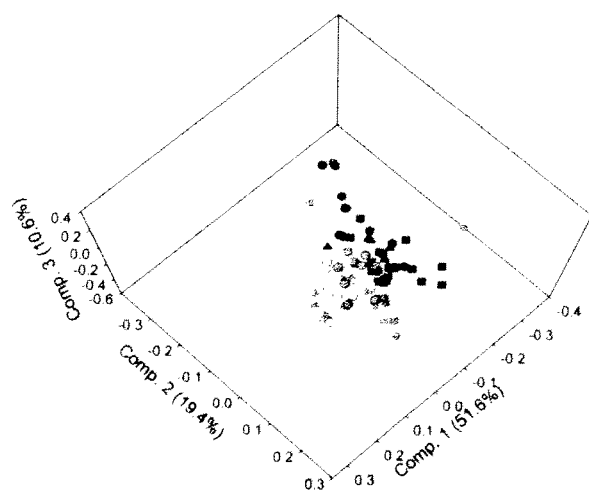


Fig. 9. Principal components analysis of the light fraction samples. All four sites are included. W.K. Kellogg Biological Station samples are squares, Lamberton samples are triangles, Hoytville samples are circles, and Wooster samples are hexagons. Time zero is white, samples incubated for 440 d are gray, and 800-d incubation are black. The percentage of the spectral variance accounted for each component is in parenthesis.

that during incubation, the clay fraction loses absorbance at the quartz overtone bands between  $1800$  and  $2000\text{ cm}^{-1}$ , and the CH deformation band between  $1270$  and  $1460\text{ cm}^{-1}$  (Fig. 12). The  $1460$  to  $1270\text{ cm}^{-1}$  region is high in the Lamberton clay fraction (Fig. 1), but is shown to contain some mineral bands in the whole soil spectra (Fig. 2). Absorbance losses at  $1730\text{ cm}^{-1}$  suggest losses of carbonyls in esters, which should be relatively easy to split during decomposition. The clay increases in absorbance at a prominent band near  $1205\text{ cm}^{-1}$ , and at the  $3400\text{ cm}^{-1}$  OH/NH band. Spectral changes of the clays are mostly the reverse of the patterns obtained during the LF incubation throughout most of the MidIR spectral range, demonstrating that LF decomposition follows a very different chemistry than the transformations of the clay fraction. Specifically the following spectral changes in the clays during incubation are opposite to the spectral changes in the LF: (i) increase in the OH/NH band at  $3400\text{ cm}^{-1}$ , (ii) decrease in the carbohydrate band at  $2200$  to  $2000\text{ cm}^{-1}$ , (iii) decrease throughout a large spectral region between  $1730$  and  $1250\text{ cm}^{-1}$  that includes bands for aromatics, aliphatics, amides, proteins, phenolics, and (iv) decrease in absorbance in the region between  $650$  and  $100\text{ cm}^{-1}$  and the peak at  $479\text{ cm}^{-1}$ . Haile-Mariam et al. (2008) showed that the clay C concentration did not change as much as the LF during the incubation, although there was a small decline in the Hoytville soil. Table 2 shows that clay has the oldest C for both corn and noncorn derived SOC, suggesting that the clay fraction can be considered very stable and highly processed compared with the rest of the size fractions. We hypothesize that the spectroscopic changes in the clay fraction are explained mostly by a change in the quality of the organic material, instead of the amount of C lost.

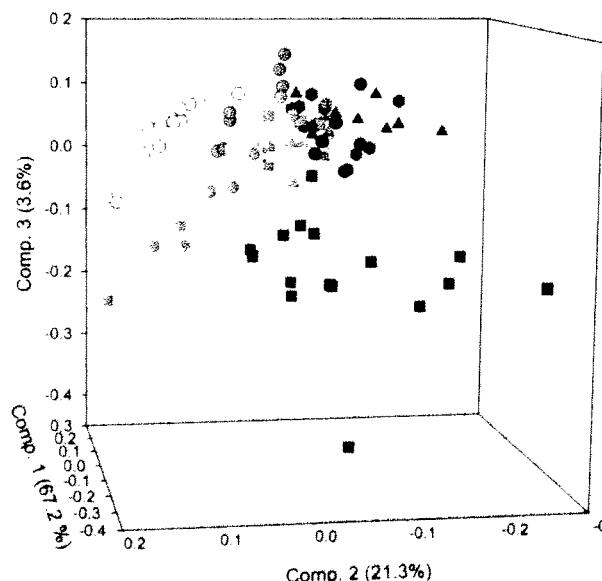


Fig. 10. Principal components analysis of the clay-sized fraction samples. All four sites are included. W.K. Kellogg Biological Station samples are squares, Lamberton samples are triangles, Hoytville samples are circles, and Wooster samples are hexagons. Time zero is white, samples incubated for 440 d are gray, and 800-d incubation are black. The percentage of the spectral variance accounted for each component is in parenthesis

There are a number of approaches for determining the molecular structure of SOM relative to its dynamics. Plante et al. (2009) analyzed soils from the same Hoytville site by using Pyrolysis-molecular beam mass spectrometry (Py-MBMS). Although, they looked at humic acid fractions and whole soils while the present study looked at particle-size fractions and whole soils, some observations can be made regarding these two studies. Both MidIR and Py-MBMS are data-rich and fast, but MidIR is nondestructive. Both techniques require extensive statistical analysis, and both give a good relation to total soil C and clearly separate soils at depth. Pyrolysis-molecular beam mass spectrometry characterizes the molecular weight of heat breakdown products. It gave good resolution of humic acid fractions and cultivated vs. grassland or forest soils. Mid-infrared relies on the vibrational absorbance of functional groups of SOM. This study showed the clear resolution of the SOM signals from particle-size fractions, which differ in the age and chemistry of organic C. One advantage of MidIR over Py-MBMS is that mineral features like clays, silicates, and carbonates can be identified. This however can also be a disadvantage until the different bands have been clearly differentiated.

The techniques are complementary and both could benefit from increased use of internal standards to help quantify the data obtained. The use of multiple techniques, on similar soil samples, that have been characterized relative to their dynamics by tracers helps to look at SOM from different perspectives and also brings out the merits of the different techniques.

Many studies have now established that MidIR with multivariate analysis is a powerful tool to develop accurate calibrations for total soil C. Clearly, infrared spectra contain wealth of information about soil C quality that can be exploited with judicious interpretation. Our results also show that MidIR spectroscopy can be used as a screening tool to quickly distinguish different soil types. Soils with different amounts of calcareous materials can also be resolved by absorbance at 2517  $\text{cm}^{-1}$ .

#### ACKNOWLEDGMENTS

We want to thank Michelle Haddix, Michael Pappas, and Brandon Peterson for all their help with the sample preparation and laboratory analyses. Thanks to Shawel Haile-Mariam for

previous research done with this sample set. This study was partially funded by a grant to E. A. Paul from the U.S. DOE, Office of Research, DE-FG03-00ER 66297. Soil analyses presented in Table 1 were carried out at the Dep. of Crop and Soil Sciences, Michigan State University. Thanks to the Ohio State University, University of

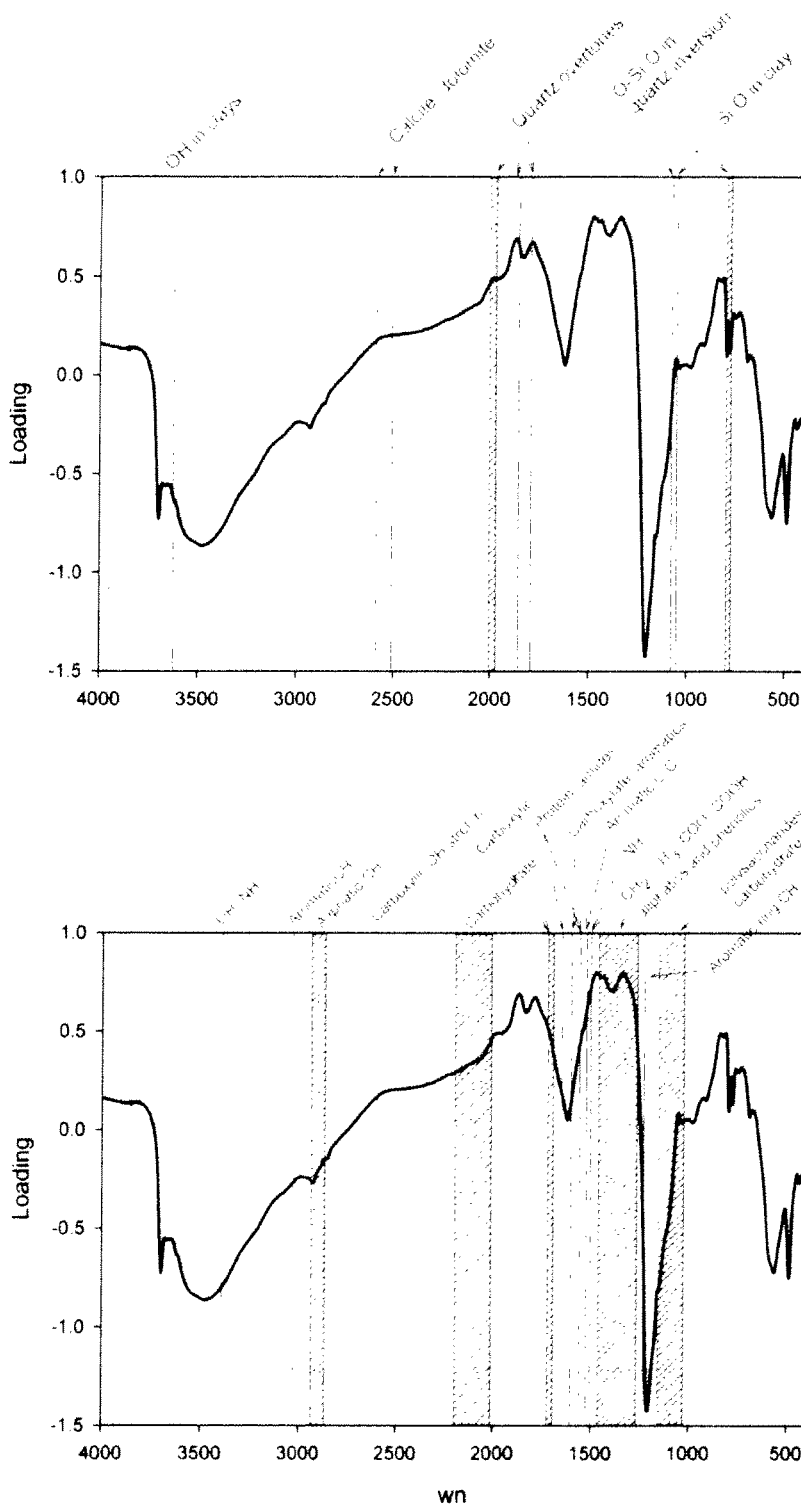


Fig. 12. Component 2 loadings for the principal components analysis shown in the clay fraction PCA in Fig. 10; wn, wavenumbers in  $\text{cm}^{-1}$ . Top graph has the mineral bands indicated, bottom graph has the organic bands.